

Multimodal Optimal Transport for Unsupervised Temporal Segmentation in Surgical Robotics

Omar Mohamed¹, Edoardo Fazzari^{*1}, Ayah Al-Naji¹, Hamdan Alhadhrami¹,
Khalfan Hableel¹, Saif Alkindi¹, and Cesare Stefanini¹

MBZUAI, Abu Dhabi, UAE

* Corresponding author: edoardo.fazzari@mbzuai.ac.ae

Abstract. Recognizing surgical phases and steps from video is a fundamental problem in computer-assisted interventions. Recent approaches increasingly rely on large-scale pre-training on thousands of labeled surgical videos, followed by zero-shot transfer to specific procedures. While effective, this strategy incurs substantial computational and data collection costs. In this work, we question whether such heavy pre-training is truly necessary. We propose Text-Augmented Action Segmentation Optimal Transport (TASOT), an unsupervised method for surgical phase and step recognition that extends Action Segmentation Optimal Transport (ASOT) by incorporating textual information generated directly from the videos. TASOT formulates temporal action segmentation as a multimodal optimal transport problem, where the matching cost is defined as a weighted combination of visual and text-based costs. The visual term captures frame-level appearance similarity, while the text term provides complementary semantic cues, and both are jointly regularized through a temporally consistent unbalanced Gromov-Wasserstein formulation. This design enables effective alignment between video frames and surgical actions without surgical-specific pretraining or external web-scale supervision. We evaluate TASOT on multiple benchmark surgical datasets and observe consistent and substantial improvements over existing zero-shot methods, including StrasBypass70 (+23.7), BernBypass70 (+4.5), Cholec80 (+16.5), and AutoLaparo (+19.6). These results demonstrate that fine-grained surgical understanding can be achieved by exploiting information already present in standard visual and textual representations, without resorting to increasingly complex pre-training pipelines. The code will be available at <https://github.com/omar8ahmed9/TASOT>.

Keywords: Surgical video understanding · Surgical Robotics · Unsupervised Learning · Vision-language.

1 Introduction

Understanding video actions at the temporal level is a fundamental task in computer vision, especially for long, untrimmed procedural videos [3]. This understanding is crucial in multiple domains, from industrial assembly lines and neuroscience to surgical procedures and robot learning [16]. In particular, surgical

robotics has emerged as a key application: segmenting surgical workflow phases and steps from video can improve intraoperative guidance, enable automated skill assessment, and support real-time autonomy or decision assistance [5, 26]. However, surgical video presents unique challenges. The visual scene is highly complex and dynamic, with frequent occlusions, camera motion, and ambiguous anatomical structures [20]. These factors make it difficult to distinguish actions based solely on visual appearance [4, 10].

Moreover, approaches that rely on fully supervised segmentation typically require dense annotations for surgical videos, which are extremely expensive, as each frame must often be labeled by a medical expert. Collecting large annotated surgical datasets is therefore laborious and time-consuming [7]. To reduce the annotation burden, most recent efforts have explored “zero-shot” or transfer-based approaches in the surgical domain [26]. Although these approaches achieve state-of-the-art performance without requiring dense annotations, they typically still rely on large pretrained networks, employ general and complex architectures that are not specifically designed to enforce temporal segment structure, and incur high computational costs [11]. In short, existing surgical video segmentation methods either demand heavy annotation effort or depend on complex pretrained models, and they do not explicitly exploit the structure of fully unsupervised temporal segmentation. Given these limitations, we ask the following question: *Is large-scale surgical pretraining truly necessary for effective temporal segmentation, or can an unsupervised approach achieve competitive performance?*

To address this question, we propose TASOT (Text-Augmented Action Segmentation Optimal Transport), an unsupervised method of surgical phase and step recognition that extends Action Segmentation Optimal Transport (ASOT) [23] by incorporating textual information generated directly from videos. Crucially, TASOT requires no task-specific supervised pretraining and no massive backbone architectures tailored to surgical data. Instead, we use modest off-the-shelf encoders for video frames and associated textual data, and let an optimal transport (OT) formulation fuse them. In other words, TASOT aligns video and text sequences within a unified framework, where a temporally consistent unbalanced Gromov–Wasserstein OT [19] formulation ensures coherent segment boundaries across both modalities.

We evaluated our model on 3 publicly available datasets, i.e., Cholec80 [20], AutoLaparo [22], and MultiBypass140 [8] from both centers. Across all datasets, TASOT consistently outperforms state-of-the-art zero-shot models in terms of F1 score, demonstrating that surgical temporal understanding can be achieved without large-scale surgical pretraining. In summary, our contributions are:

- We propose the first multimodal OT-based framework for unsupervised temporal segmentation in the surgical domain, introducing a formulation that integrates visual and textual cues within a unified optimal transport objective, regularized by temporally consistent Gromov–Wasserstein constraints.
- We demonstrate state-of-the-art performance in unsupervised surgical temporal segmentation, consistently outperforming existing zero-shot methods on F1 scores across multiple benchmark datasets.

2 Related Work

2.1 Surgical Temporal Segmentation

Early surgical workflow recognition methods relied on fully supervised learning with dense frame-level annotations. For instance, EndoNet [20] introduced a deep CNN architecture for phase recognition in laparoscopic videos. Subsequent approaches incorporated recurrent architectures to model temporal dependencies, followed by Temporal Convolutional Networks (TCNs), including TeCNO [2] and MTMS-TCN [12], to improve temporal consistency and enable joint phase and step recognition. More recently, transformer-based models [9, 19] have been proposed to capture long-range temporal dependencies in surgical workflows. Despite achieving strong performance, the fully supervised approach remains dependent on costly and labor-intensive frame-level annotations [8].

In order to reduce annotation work, recent video–language pretraining approaches learn joint visual–text representations for zero-shot surgical recognition. Inspired by large-scale contrastive models such as CLIP [11] and instructional video pretraining frameworks such as MIL-NCE [10], surgical adaptations have emerged to leverage domain-specific video–text corpora. SurgVLP [26] aligns surgical videos with narrated transcripts via contrastive learning, while HecVL [25] introduces hierarchical video–text supervision to enable zero-shot phase recognition across procedures. PeskaVLP [24] further enhances cross-modal alignment using large language model augmentation and procedural matching objectives, reporting strong zero-shot performance. Although these methods reduce annotation requirements at deployment, they rely on very large curated surgical video–text corpora and heavyweight multimodal Transformers, resulting in substantial pretraining cost and computational complexity.

2.2 Unsupervised Temporal Segmentation

In general, unsupervised temporal action segmentation aims to partition untrimmed videos into coherent segments without frame-level annotations [3]. Early approaches learn frame embeddings and cluster them under temporal regularization [13, 14], later refined through reconstruction [21] or discriminative embedding objectives [17]. More recently, Optimal Transport (OT) has provided a principled framework for joint representation learning and pseudo-label assignment. In particular, ASOT [23] formulates segmentation as an unbalanced Gromov–Wasserstein OT problem without predefined action ordering, achieving strong general-domain performance. HVQ [16] further improves short-action detection via hierarchical vector quantization, but its codebook-based formulation does not explicitly couple representation learning with clustering as in OT-based alignment. Nevertheless, existing OT-based approaches operate purely on visual features. To date, multimodal textual cues have not yet been integrated into an unsupervised OT framework for surgical temporal segmentation.

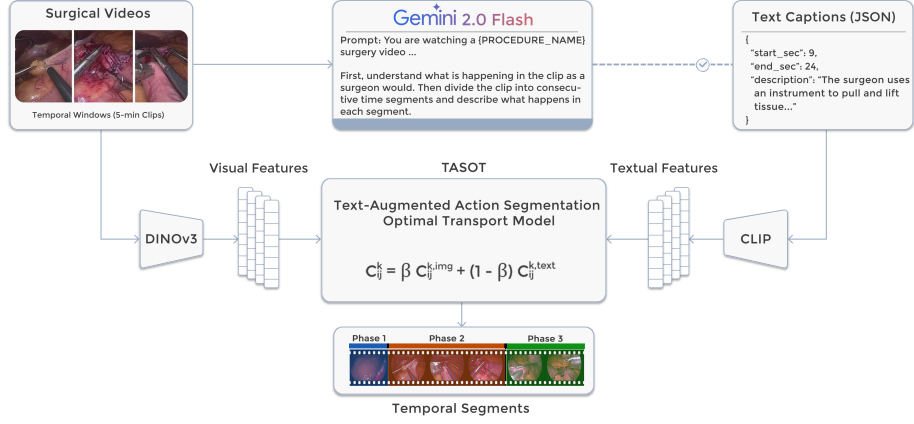


Fig. 1. Overview of TASOT Surgical videos are divided into temporal windows and processed by a vision–language model to generate structured temporal captions. Visual features (DINOv3) and temporally aligned textual features (CLIP) are integrated within the TASOT model, where a weighted multimodal cost is used for unsupervised surgical temporal segmentation.

3 Methods

We introduce **TASOT (Text-Augmented Action Segmentation Optimal Transport)**, a multimodal extension of ASOT [23] for unsupervised temporal segmentation of long surgical videos. As illustrated in Fig. 1, TASOT extends the original optimal transport formulation by: (i) generating dense temporal captions from raw videos, (ii) encoding captions with a text encoder (CLIP) [11] and frames with a visual encoder (DINOv3) [15], and (iii) introducing a multimodal cost that integrates visual-to-prototype and text-to-prototype similarities within a unified transport objective. The resulting transport plan provides pseudo-labels for representation learning within a self-training framework.

3.1 Captioning Pipeline

Each surgical video v of duration T seconds are divided into non-overlapping windows of fixed length W (default $W=300$ s):

$$w_m = v[s_m, e_m), \quad s_m = mW, \quad e_m = \min((m+1)W, T), \quad (1)$$

where s_m and e_m denote the start and end times of the m -th window w .

For each window clip, Gemini 2.0 Flash [6] generates consecutive temporal segments with natural language descriptions:

$$\mathcal{S}_m = \left\{ (\tau_j^{(m)}, \tau_{j+1}^{(m)}, \text{text}_j^{(m)}) \right\}_{j=1}^{J_m}, \quad 0 = \tau_1^{(m)} < \dots < \tau_{J_m+1}^{(m)} = |w_m|. \quad (2)$$

To fix window-local times, we converted them to global video time simply by applying:

$$t_{j,\text{start}}^{(m)} = s_m + \tau_j^{(m)}, \quad t_{j,\text{end}}^{(m)} = s_m + \tau_{j+1}^{(m)}. \quad (3)$$

Finally, window-level segments are merged and temporally ordered to form the video-level caption set.

3.2 TASOT Framework

Firstly, a feature extraction phase was performed. Videos are sampled at 1 fps, consistent with surgical workflow annotations, then, each selected frame is encoded using DINOv3 [15] to obtain visual features x_t^{img} . Similarly, caption segments are embedded using CLIP [11], producing text features e_j . Each frame at time t is assigned the embedding of the caption segment whose temporal interval contains t , yielding temporally aligned textual features x_t^{text} .

Following [23], we learn K normalized prototypes $A = \{a_k\}_{k=1}^K$ in a latent space for optimal transport-based segmentation. While ASOT employs a single projection head over visual features, TASOT extends this formulation by introducing modality-specific projection heads for both visual and textual streams.

Given aligned features x_t^{img} and x_t^{text} , we project them into a shared latent space and perform normalization, obtaining z_t^{img} and z_t^{text} .

Using the normalized embeddings and prototypes, we define and compute a newly modality-specific cosine-distance costs:

$$C_{i,k}^{\text{img}} = 1 - \langle z_i^{\text{img}}, a_k \rangle, \quad C_{i,k}^{\text{text}} = 1 - \langle z_i^{\text{text}}, a_k \rangle. \quad (4)$$

Our cost matrix is defined as a weighted combination: Then, we defined our cost matrix as the following weighted combination:

$$C_{i,k} = \beta C_{i,k}^{\text{img}} + (1 - \beta) C_{i,k}^{\text{text}}, \quad (5)$$

where $\beta \in [0, 1]$ controls the visual-text trade-off.

Following ASOT [23], we incorporate the temporal prior into the cost matrix to encourage monotonic alignment between temporal indices and action prototypes.

Finally, using the multimodal cost matrix, we compute a soft transport plan T using the original ASOT solver, which incorporates temporal regularization and optional unbalanced constraints. The resulting transport assignments serve as pseudo-labels for representation learning. Cluster probabilities are computed from the fused embedding and optimized via cross-entropy against the OT assignments.

4 Experimental Results and Discussion

4.1 Experimental Setup

We evaluate TASOT on three public surgical datasets: Cholec80 [20] (80 videos, 7 phases), AutoLaparo [22] (21 videos, 7 phases), and MultiBypass140 [8] (140 videos from Strasbourg and Bern, annotated with 12 phases and 46 steps). For MultiBypass140, results are reported separately for each center following the official zero-shot evaluation protocol. Predicted clusters are aligned with ground-truth labels using Hungarian matching [23]. We report segmental F1 score [3] as the primary metric for fair comparison with prior work.

Table 1. Phase and step recognition results on Cholec80 [20], AutoLaparo [22], and MultiBypass140 (BernByPass70, StrasByPass70) [8]. Best results are in **bold**.

Method	Cholec80	AutoLaparo	BernByPass70		StrasByPass70	
	Phase F1	Phase F1	Phase F1	Step F1	Phase F1	Step F1
<i>Zero-shot Methods</i>						
MIL-NCE [10]	7.3	7.9	2.1	—	3.1	—
CLIP-SVL [11]	19.6	16.2	7.1	—	8.6	—
SurgVLP [26]	24.4	16.6	7.2	—	6.9	—
HecVL [25]	26.3	18.9	13.6	—	18.3	—
PeskaVLP [24]	34.2	23.6	22.6	—	28.6	—
<i>Unsupervised Method</i>						
TASOT (Ours)	50.7	43.2	27.1	23.0	52.3	30.7

4.2 State-of-the-Art Comparisons

We compare TASOT against recent zero-shot surgical video–language models, as shown in Table 1. TASOT substantially improves performance across all datasets, outperforming the strongest zero-shot baseline by +16.5 on Cholec80 and +19.6 on AutoLaparo. On MultiBypass140, TASOT achieves 52.3 on StrasByPass70 (+23.7) and 27.1 on BernByPass70 (+4.5), demonstrating robustness across various surgical datasets. It further attains 30.7 and 23.0 for step recognition on StrasByPass70 and BernByPass70, respectively, indicating effectiveness on finer-grained temporal segmentation, however no results are available for zero-shot, probably the difficulty of the problem. Furthermore, these results show that our method enables very strong surgical workflow understanding without requiring large-scale surgical pretraining.

4.3 Ablation Study

We conduct ablations on MultiBypass140 to assess how different feature contribute, test different text encoders and the understand the influence of having a fixed number of clusters.

To understand the importance of each feature, we tested TASOT considering only vision features, text features and a concatenation of them, instead of using our multimodal cost for their integration. Results are shown in Table 2 suggesting

Table 2. TASOT ablation study results. Best results are in **bold**.

Model	BernByPass70		StrasByPass70	
	Phase F1	Step F1	Phase F1	Step F1
Visual-only	27.9	20.3	51.3	27.9
Text-only	18.2	7.98	26.3	9.39
Feature concatenation	27.4	14.3	50.4	21.2
TASOT	27.1	23.0	52.3	30.7

Table 3. Backbone analysis on MultiBypass140. \parallel indicates feature concatenation.

Visual Encoder	Text Encoder	BernByPass70		StrasByPass70	
		Phase F1	Step F1	Phase F1	Step F1
DINOv3	CLIP	27.1	23.0	52.3	30.7
DINOv3	Gemma	26.7	22.4	49.2	29.9
DINOv3	Gemma \parallel CLIP	26.6	22.1	50.3	30.6

Table 4. Analysis on using a video-specific number of clusters for MultiBypass140 and comparison to supervised models. Best result for unsupervised in **bold**.

Method	BernByPass70		StrasByPass70	
	Phase F1	Step F1	Phase F1	Step F1
<i>Unsupervised Methods</i>				
TASOT	27.1	23.0	52.3	30.7
TASOT (k -specific)	49.7	48.8	56.9	52.4
<i>Supervised Methods</i>				
TeCNO [8]	59.2	47.5	80.7	58.1
MTMS-TCN [8]	62.4	47.9	79.8	57.3

that our multimodal cost solution is the best demonstrating that our integration of multimodal cues in the OT objective helps improving temporal segmentation.

To analyze the impact of the textual encoding, we substituted CLIP with Gemma [18] following current contrastive learning approaches [1] and we report the results in Table 3. DINOv3 combined with CLIP text embeddings achieves the highest performance for both phase and step recognition, outperforming the Gemma-based variants. This suggests that CLIP provides stronger semantic alignment within the OT framework and our use to introduce DINOv3 for the extraction of image features.

Finally, we investigated the impact of the number of clusters provided as input to our model, which varies across videos. Figure 2 presents qualitative examples of the temporal segmentation produced by TASOT. The model generates coherent phase-level segmentations with sharp, well-aligned boundaries that closely follow the ground truth annotations, although step-level segmentation remains more challenging due to its finer temporal granularity resulting moderately fragmented. By looking at the result, we believe this is correlated to the number of clusters provided, more than what actually are presented in the videos. In fact, in our primary experiments, the number of clusters k is fixed according to total possible classes. Consequently, TASOT predicts exactly k segments per procedure, which may restrict its flexibility in adapting to video-specific variability. To better assess the effect of this constraint, we conducted additional experiments on the MultiBypass140 dataset, adapting K to match the actual number of classes in each individual video. The results are reported in Table 4. This strategy leads to a substantial improvement in overall performance, partic-

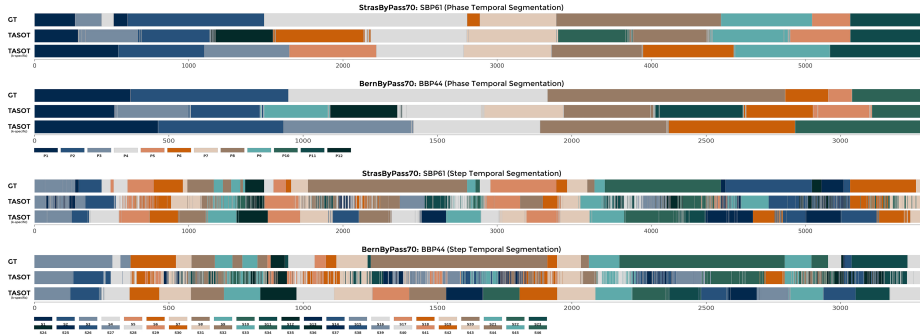


Fig. 2. Qualitative results We display the ground-truth (GT) and the results of TASOT (Ours) from the MultiByPass140 dataset.

ularly for step-level segmentation. Specifically, performance on BernBypass140 increases from 23.0 to 48.8, surpassing even the supervised baseline, while results on StrasBypass140 improve from 30.7 to 52.4, nearly closing the gap with the unsupervised upper bound.

5 Conclusion

We introduced TASOT, a fully unsupervised multimodal optimal-transport framework for temporal segmentation that extends ASOT by integrating visual and temporally aligned textual cues within a unified unbalanced Gromov–Wasserstein formulation. TASOT consistently outperforms recent zero-shot surgical video-language baselines on Cholec80, AutoLaparo, and MultiBypass140 for phase and step recognition, demonstrating that fine-grained workflow understanding can be achieved without large-scale surgical-specific pretraining. Ablation studies highlight the necessity of cost-level multimodal fusion over unimodal variants and feature concatenation, while qualitative results confirm coherent phase boundaries and robust temporal structure, with step segmentation remaining inherently more challenging due to finer granularity.

A relevant aspect to consider is the use of a fixed number of clusters k , defined according to the total number of annotated classes. While this setting follows the standard experimental configuration, our analysis indicates that not all classes are necessarily present in every individual video. Consequently, constraining the model to predict a fixed number of segments may reduce its ability to fully adapt to video-specific variability. Enabling adaptive estimation of the number of clusters therefore represents a natural and promising direction for future work. Finally, and importantly, TASOT is not restricted to surgical robotics and can generalize to other long, untrimmed procedural video domains where aligned textual cues are available.

Acknowledgments. This study was funded by X (project number Y).

Disclosure of Interests. Authors have no competing interests.

References

1. Chen, D., Shukor, M., Moutakanni, T., Chung, W., Yu, J., Kasarla, T., Bolourchi, A., LeCun, Y., Fung, P.: Vl-jepa: Joint embedding predictive architecture for vision-language. arXiv preprint arXiv:2512.10942 (2025)
2. Czempiel, T., Paschali, M., Keicher, M., Simson, W., Feussner, H., Kim, S.T., Navab, N.: Tecno: Surgical phase recognition with multi-stage temporal convolutional networks. In: International conference on medical image computing and computer-assisted intervention. pp. 343–352. Springer (2020)
3. Ding, G., Sener, F., Yao, A.: Temporal action segmentation: An analysis of modern techniques. *IEEE Transactions on Pattern Analysis and Machine Intelligence* **46**(2), 1011–1030 (2024). <https://doi.org/10.1109/TPAMI.2023.3327284>
4. Fazzari, E., Romano, D., Falchi, F., Stefanini, C.: Artemis: animal recognition through enhanced multimodal integration system. *International Journal of Machine Learning and Cybernetics* **16**(9), 5877–5892 (2025)
5. Fazzari, E., Stefanini, C.: Deep reinforcement learning for surgical robotics with state and image information: A survey. *Research Square* (2026). <https://doi.org/10.21203/rs.3.rs-8621244/v1>
6. Google DeepMind: Gemini 2.0 flash model card. Tech. rep., Google (April 2025), available at <https://modelcards.withgoogle.com/assets/documents/gemini-2-flash.pdf>
7. Hashemi, N., Svendsen, M.B.S., Bjerrum, F., Rasmussen, S., Tolsgaard, M.G., Friis, M.L.: Acquisition and usage of robotic surgical data for machine learning analysis. *Surgical Endoscopy* **37**(8), 6588–6601 (2023)
8. Lavanchy, J.L., Ramesh, S., Dall’Alba, D., Gonzalez, C., Fiorini, P., Müller-Stich, B.P., Nett, P.C., Marescaux, J., Mutter, D., Padoy, N.: Challenges in multi-centric generalization: phase and step recognition in roux-en-y gastric bypass surgery. *International journal of computer assisted radiology and surgery* **19**(11), 2249–2257 (2024)
9. Liu, Y., Boels, M., Garcia-Peraza-Herrera, L.C., Vercauteren, T., Dasgupta, P., Granados, A., Ourselin, S.: Lovit: Long video transformer for surgical phase recognition. *Medical Image Analysis* **99**, 103366 (2025)
10. Miech, A., Alayrac, J.B., Smaira, L., Laptev, I., Sivic, J., Zisserman, A.: End-to-end learning of visual representations from uncurated instructional videos. In: Proceedings of the IEEE/CVF conference on computer vision and pattern recognition. pp. 9879–9889 (2020)
11. Radford, A., Kim, J.W., Hallacy, C., Ramesh, A., Goh, G., Agarwal, S., Sastry, G., Askell, A., Mishkin, P., Clark, J., et al.: Learning transferable visual models from natural language supervision. In: International conference on machine learning. pp. 8748–8763. PmLR (2021)
12. Ramesh, S., Dall’Alba, D., Gonzalez, C., Yu, T., Mascagni, P., Mutter, D., Marescaux, J., Fiorini, P., Padoy, N.: Multi-task temporal convolutional networks for joint recognition of surgical phases and steps in gastric bypass procedures. *International journal of computer assisted radiology and surgery* **16**(7), 1111–1119 (2021)
13. Sarfraz, S., Murray, N., Sharma, V., Diba, A., Van Gool, L., Stiefelhagen, R.: Temporally-weighted hierarchical clustering for unsupervised action segmentation. In: Proceedings of the IEEE/CVF Conference on Computer Vision and Pattern Recognition. pp. 11225–11234 (2021)

14. Sener, F., Yao, A.: Unsupervised learning and segmentation of complex activities from video. In: Proceedings of the IEEE conference on computer vision and pattern recognition. pp. 8368–8376 (2018)
15. Siméoni, O., Vo, H.V., Seitzer, M., Baldassarre, F., Oquab, M., Jose, C., Khali-dov, V., Szafraniec, M., Yi, S., Ramamonjisoa, M., et al.: Dinov3. arXiv preprint arXiv:2508.10104 (2025)
16. Spurio, F., Bahrami, E., Francesca, G., Gall, J.: Hierarchical vector quantization for unsupervised action segmentation. In: Proceedings of the AAAI Conference on Artificial Intelligence. vol. 39, pp. 6996–7005 (2025)
17. Swetha, S., Kuehne, H., Rawat, Y.S., Shah, M.: Unsupervised discriminative embedding for sub-action learning in complex activities. In: 2021 IEEE International Conference on Image Processing (ICIP). pp. 2588–2592. IEEE (2021)
18. Team, G., Mesnard, T., Hardin, C., Dadashi, R., Bhupatiraju, S., Pathak, S., Sifre, L., Rivière, M., Kale, M.S., Love, J., et al.: Gemma: Open models based on gemini research and technology. arXiv preprint arXiv:2403.08295 (2024)
19. Titouan, V., Flamary, R., Courty, N., Tavenard, R., Chapel, L.: Sliced gromov-wasserstein. *Advances in Neural Information Processing Systems* **32** (2019)
20. Twinanda, A.P., Shehata, S., Mutter, D., Marescaux, J., de Mathelin, M., Padoy, N.: Endonet: A deep architecture for recognition tasks on laparoscopic videos. *IEEE Transactions on Medical Imaging* **36**(1), 86–97 (2017). <https://doi.org/10.1109/TMI.2016.2593957>
21. VidalMata, R.G., Scheirer, W.J., Kukleva, A., Cox, D., Kuehne, H.: Joint visual-temporal embedding for unsupervised learning of actions in untrimmed sequences. In: Proceedings of the IEEE/CVF Winter Conference on Applications of Computer Vision. pp. 1238–1247 (2021)
22. Wang, Z., Lu, B., Long, Y., Zhong, F., Cheung, T.H., Dou, Q., Liu, Y.: Autolaparo: A new dataset of integrated multi-tasks for image-guided surgical automation in laparoscopic hysterectomy. In: International Conference on Medical Image Computing and Computer-Assisted Intervention. pp. 486–496. Springer (2022)
23. Xu, M., Gould, S.: Temporally consistent unbalanced optimal transport for unsupervised action segmentation. In: Proceedings of the IEEE/CVF Conference on Computer Vision and Pattern Recognition (CVPR). pp. 14618–14627 (June 2024)
24. Yuan, K., Navab, N., Padoy, N., et al.: Procedure-aware surgical video-language pretraining with hierarchical knowledge augmentation. *Advances in Neural Information Processing Systems* **37**, 122952–122983 (2024)
25. Yuan, K., Srivastav, V., Navab, N., Padoy, N.: Hecvl: Hierarchical video-language pretraining for zero-shot surgical phase recognition. In: International Conference on Medical Image Computing and Computer-Assisted Intervention. pp. 306–316. Springer (2024)
26. Yuan, K., Srivastav, V., Yu, T., Lavanchy, J.L., Marescaux, J., Mascagni, P., Navab, N., Padoy, N.: Learning multi-modal representations by watching hundreds of surgical video lectures. *Medical Image Analysis* p. 103644 (2025)